Carbohydrate Polymers 81 (2010) 906–910

Contents lists available at ScienceDirect

Carbohydrate Polymers

journal homepage: www.elsevier.com/locate/carbpol

Magnetic chitosan/iron (II, III) oxide nanoparticles prepared by spray-drying

Hsin-Yi Huang[a], Yeong-Tarng Shieh[b], Chao-Ming Shih[a], Yawo-Kuo Twu[a,*]

[a] Department of Bioindustry Technology, Dayeh University, Changhua 51591, Taiwan, ROC
[b] Department of Chemical and Materials Engineering, National University of Kaohsiung, Kaohsiung 81148, Taiwan, ROC

ARTICLE INFO

Article history:
Received 12 August 2009
Received in revised form 12 February 2010
Accepted 7 April 2010
Available online 14 April 2010

Keywords:
Chitosan
Spray-drying
Iron oxide
Magnetization
Superparamagnetic property

ABSTRACT

Chitosan/iron (II, III) oxide nanoparticles with various ratios of chitosan/iron (CS1/Fe4, CS2/Fe4 and CS3/Fe4) were prepared by a spray-drying method. Atomic absorption spectrometry (AAS), Fourier transform infrared spectroscopy (FTIR), and X-ray diffraction (XRD) spectrometry data confirm that magnetic crystalline Fe_3O_4 interacts with chitosan and distributes in the chitosan matrix. Field emission scanning electron microscopy (FESEM) micrographs indicate that nanoparticles so prepared have a good sphericity and a rough surface morphology. The average diameters of CS1/Fe4, CS2/Fe4, and CS3/Fe4 were 236, 379 and 417 nm, respectively. Superconducting quantum interference device (SQUID) results indicate that the highest saturation magnetization of magnetic nanoparticles is about 27.91 emu/g. The hysteresis loop of the samples shows that all samples manifest zero coercivity and zero remanence, which infers that each of the samples has a superparamagnetic property. Dynamic light scattering (DLS) data show that the zeta potential of samples is higher than 45 mV, indicating that the samples can steadily distribute in water.

1. Introduction

Chitosan is a polysaccharide obtained from the deacetylation of chitin. It is a biomaterial with excellent features and is highly valued for its medical applications. Chitosan has many advantages, including being non-toxic, biocompatible, and biodegradable (Arvanitoyannis, 1999; Shahidi, Arachchi, & Jeon, 1999; Yen, Yang, & Mau, 2008). Chitosan, chitosan derivatives, and their composites can be produced into colloids and membranes, and can be used to control medicine release as well as tissue engineering (Arvanitoyannis, Nakayama, & Aiba, 1998; Hong, Liu, & Wu, 2009; Twu, Huang, Chang, & Wang, 2003; Wang, Liu, Han, & Yang, 2009; Yen et al., 2008).

In recent years, magnetic nanoparticles have been extensively discussed and studied, especially iron oxide nanoparticles (Gupta & Gupta, 2005). Superparamagnetic iron oxide nanoparticles include γ-Fe_2O_3 and Fe_3O_4, among others (Chatterjee, Haik, & Chen, 2003; Kim, Ahn, & Lee, 2007; Neuberger, Schöpf, Hofmann, Hofmann, & Rechenberg, 2005; Sun, Ma, Zhang, & Gu, 2004). These can be produced using the bulk solution method (Sun et al., 2004), the sol–gel method (Jotania, Khomane, Chauhan, Menon, & Kulkarni, 2008), the aerosol/vapour (pyrolysis) method (Racka, Gich, Waniewska, Roig, & Molins, 2005), the gas deposition method (Rellinghaus, Stappert, Acet, & Wassermann, 2003), and the microemulsion method (Jia, Yujun, Yangcheng, Jingyu, & Guangsheng, 2006; Jotania et al., 2008). Magnetic iron oxide nanoparticles have features of superparamagnetism, high coercive force, and small-size effect (Huber, 2005; Neuberger et al., 2005). Their excellent biosafety and biocompatibility have drawn the attention of researchers engaged in biological and medical studies (Ito, Shinkai, Honda, & Kobayashi, 2005; Xu & Sun, 2007). Relevant applications include: drug delivery (Berry & Curtis, 2003), cell separation and cellular labeling (Gupta & Curtis, 2004), enzyme immobilization (Hong, Gong, Xu, Dong, & Yao, 2007), magnetic resonance imaging (Yan, Robinson, & Hogg, 2007), and hyperthermia applications (Park et al., 2005).

A magnetic composite particle features the combination of two or more materials into a single particle. Its material choice and application are more extensive than particles of single ingredient (Xu & Sun, 2007; Zhang, Zhang, Wang, & Zeng, 2007). It uses magnetic materials to mix or combine other materials to change the particles' various properties, such as: surface electrification, catalytic activity, chemical reactivity, reaction selectivity, stability, solvency, and biocompatibility (Berry & Curtis, 2003; Ito et al., 2005; Kim, Zhang, Voit, Rao, & Muhammed, 2001; Storm, Belliot, Daemen, & Lasic, 1995). Chitosan composite particles can be produced using the core–shell methodology and organic–inorganic coating system (Carpenter, 2001; Donadel et al., 2008). The particles produced are mostly at the micro-level. For example, Kim et al. produced magnetic chitosan particles between 100 μm and 150 μm (Kim et al., 2007), while Denkbaş et al. produced magnetic chitosan particles between 100 μm and 250 μm (Denkbaş, Kiliçay, Birlikseven, & Öztürk, 2002). Similarly, Donadel et al. produced micro-level magnetic chitosan particles by spray-drying (Donadel et al., 2008). This

* Corresponding author. Tel.: +886 4 851319.
E-mail address: poly2001@mail.dyu.edu.tw (Y.-K. Twu).

0144-8617/$ – see front matter © 2010 Elsevier Ltd. All rights reserved.
doi:10.1016/j.carbpol.2010.04.003

paper describes the preparation of magnetic chitosan/iron (II, III) oxide nanoparticles by means of spray-drying.

2. Experimental method

2.1. Materials and methods

Chitosan (degree of deacetylation = 85%, M_v = 1780 kDa) was supplied by Cabco Co. (Taiwan). Ferric chloride hexahydrate (98%), ferrous chloride tetrahydrate (99.9%), and ferriferrous oxide (99.99%) were purchased from Sigma–Aldrich Fine Chemicals (USA). Acetic acid (99.5%) and sodium hydroxide (97%) were obtained from Katayama Chemical Co. (Japan). The water used in this experiment was purified by a double deionization of reverse osmosis water. All chemicals and other analytic grade chemicals were used without further purification.

2.2. Preparation of magnetic chitosan/iron (II, III) oxide suspensions

To evaluate the effect of chitosan content in the alkaline chitosan suspension on the formation of magnetic particles, the molar ratios of the chitosan-repeating units to the iron atoms were set to 1:4, 2:4 and 3:4. Three solutions of 0.5, 1 and 1.5 (w/v) chitosan, respectively, were prepared in an aqueous solution made of acetic acid (500 mL, 1% (w/v)). Each solution was added into 0.5 N of aqueous sodium hydroxide solution (345 mL), solidified, and regenerated into particles through homogenization with the use of a homogenizer (Art MICCRA D-8) at 17500 rpm. Thus, milk-like alkaline chitosan suspensions with pH > 14 were obtained (marked as CS1, CS2, and CS3). Each 250 mL solution of $FeCl_3{\cdot}6H_2O$ (0.333 M) and $FeCl_2{\cdot}4H_2O$ (0.166 M) was added into CS1, CS2 and CS3, each of which were homogenized at 19500 rpm. Black suspensions with pH ~ 10 were obtained during the homogenization process conducted in approximately 10 min. Suspensions were washed several times with deionized water until the pH decreased to 7, after which brown suspensions were finally obtained.

2.3. Preparation of magnetic nanoparticles

In a typical preparation process of magnetic chitosan/iron oxide nanoparticles, the brown suspension was adjusted to 2 L by adding water and then spray dried. The spray-drying setup used in this study has been described in a previous report (Shih, Twu, & Shieh, 2006). The spray-drying conditions in the preparation of magnetic nanoparticles were as follows: the sample feeding rate was 25 mL/min, highly pressurized air was 4 kgf/cm^2, and the hot airflow rate was 600 L/min; the inlet and outlet temperatures of the drying chamber were at 180 °C and 68 °C, respectively. An electrostatic precipitator (ESP) was connected to the exit point of the spray-drier to help collect the particles. Based on the molar ratio of the chitosan-repeating units to the iron atoms, the obtained nanoparticles were CS1/Fe4, CS2/Fe4 and CS3/Fe4, respectively.

2.4. Characterization

The iron content in the chitosan/iron (II, III) oxide nanoparticles was determined by atomic absorption spectrometry (AAS, GBC 932). Fourier transform infrared spectroscopy (FTIR, SHIMADZU 8400S) was used to reassess the changes induced by the iron oxide on some properties of the chitosan composites. The crystal structure of the iron oxide distributed in the chitosan matrix was determined with X-ray diffraction (XRD, RIGAKU D/Max-2500) using Cu K_α radiation at 40 kV and 50 mA. The sample was scanned from 5° to 90° at 2θ. The surface morphology of the particles was observed by a JEOL JSM-1200EX II field emission scanning electron microscopy (FESEM). The size of the particles was measured from the enlarged FESEM micrographs by counting at least 200 individual particles from different regions on a film. The magnetic property of the magnetic particles was evaluated using a superconducting quantum interference device (SQUID, BRUKER DRX-300 NMR). Dynamic light scattering (DLS, MALVERN Zatasizer Nano-ZS) was used for zeta potential and hydrodynamic diameter measurements, which provided information on the stability of the hydrated particles in pure water.

3. Result and discussion

3.1. Magnetic chitosan/iron (II, III) oxide suspension

In the preliminary studies, the molar ratios of the chitosan-repeating units to the iron atoms were set to 1:2, 2:2 and 3:2, respectively. In view of the high chitosan content and the low saturated magnetization obtained, these ratios were not suitable for future application. In this study, the iron content was doubled. Meanwhile, to compare the influence of chitosan content on products, the molar ratios of the chitosan-repeating units to the iron atoms were set to 1:4, 2:4 and 3:4, respectively. In preparing the chitosan/iron (II, III) oxide suspension, drops of the mixture of the Fe^{3+} and Fe^{2+} solution were added into the alkaline chitosan suspension during high-speed homogenization. In the process, the suspension turned black. Afterwards, as the black suspension was repeatedly washed for neutralization, its color gradually became paler until a brown suspension was finally obtained. In Fig. 1, it can be seen that the magnet was placed between two bottles of the chitosan/iron oxide suspension, and the brown particles were attracted by the magnet. The chitosan/iron oxide particles converged rapidly around the magnet within 1 min. This result validated the assumption that the chitosan/iron (II, III) oxide suspension would manifest ferrofluid features.

3.2. Composition and structure of chitosan/iron (II, III) oxide nanoparticles

The CS1/Fe4, CS2/Fe4, and CS3/Fe4 were dissolved in the hydrochloric acid. The technique of AAS was used for finding the molar ratio of the chitosan-repeating units to the iron atoms in the nanoparticles. The content of iron was measured, after which the molar ratios of the chitosan-repeating units to the iron atoms were calculated. The analytic result is shown in Table 1. Along with the increase of chitosan in the samples, the total content of the iron decreased. Given that the iron content in the samples was higher

Fig. 1. Chitosan/iron (II, III) oxide suspension with ferrofluid property.

Table 1
Iron content and molar ratio of chitosan-repeating units/iron atoms resulted from atomic absorption spectrometry analysis of magnetic chitosan/iron (II, III) oxide nanoparticles.

Samples	Theoretical iron content (%)[a]	Found iron content (%)[b]	Theoretical molar ratio of chitosan-repeating units/iron atoms	Calculated molar ratio of chitosan-repeating units/iron atoms
CS1/Fe4	47.53	58.42	1/4	1/8.8
CS2/Fe4	35.40	42.10	1/2	1/2.9
CS3/Fe4	28.19	30.56	1/1.33	1/1.5

[a] Mass percentage = (iron mass/total mass) × %.
[b] Data were obtained from calculation of AAS results.

than in theoretical calculation, this study inferred that some low molecular weight chitosan was lost during the washing process. This could have been the result of hydrolysis during the preparation of the chitosan suspension, as well as the composite suspension. In sample CS1/Fe4, the molar ratio of the chitosan-repeating units to the iron atoms was 1:8.8. This indicated that each chitosan-repeating unit interacted with 8.8 iron atoms or 2.9 Fe_3O_4. These results implied that chitosan has strong chelation ability or there was the possibility that Fe_3O_4 had already been crystallized and distributed in the chitosan matrix. This result could be certified by XRD.

FTIR provides information about functional groups and bonding structures. Fig. 2 shows a comparison between FTIR spectra on (a) pure Fe_3O_4, (b) chitosan, and (c) CS1/Fe4. The CS1/Fe4 spectrum (Fig. 2c) exhibited characteristic absorption bands of the functional groups of the chitosan at 1647 cm^{-1}, 1552 cm^{-1}, and 1379 cm^{-1}. However, the chitosan spectrum (Fig. 2b) displayed absorption bands located at 1652 cm^{-1}, which could be attributed to amide I band, at 1591 cm^{-1} resulting from NH_2 deformation, and at 1380 cm^{-1} corresponding to the CN axial deformation of the amide group. From this analysis, it could be concluded that the amide and amine deformation bands of CS1/Fe4 shifted to lower wavenumbers. This indicated a complexation, further suggesting that the amide and/or amine groups could be coordinated to the iron ions. The absorption bands of the iron (II, III) oxides, which appeared at 579 cm^{-1} and 593 cm^{-1} (Fig. 2a and c), were assigned to Fe–O deformation in the octahedral and tetrahedral sites.

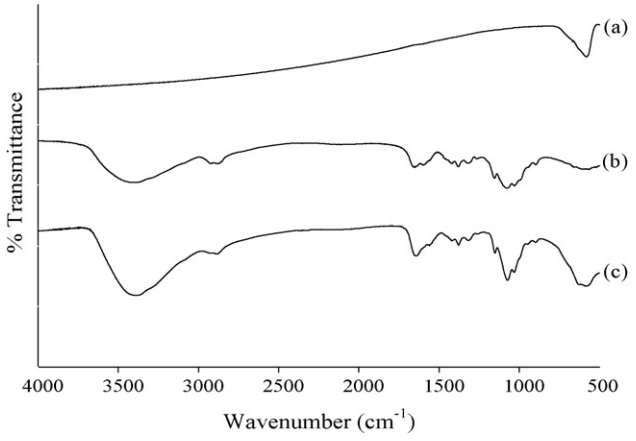

Fig. 2. FTIR absorption spectra: (a) Fe_3O_4; (b) chitosan; and (c) CS1Fe4.

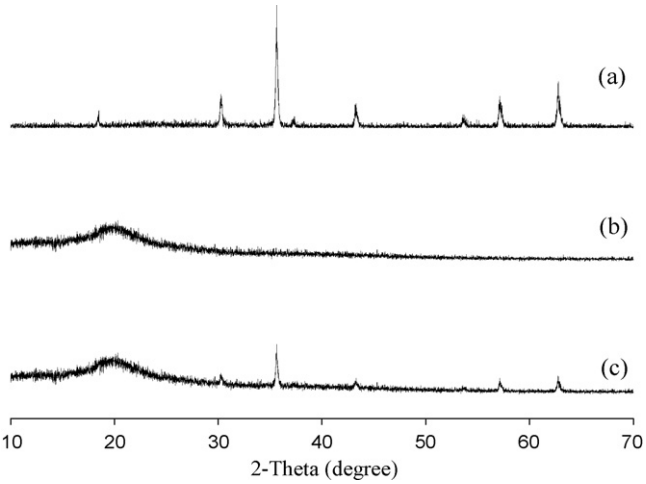

Fig. 3. X-ray diffraction patterns: (a) Fe_3O_4; (b) chitosan; and (c) CS1Fe4.

The XRD method was used to identify the crystal structure of the iron oxide dispersed in the chitosan matrix. The XRD patterns of (a) Fe_3O_4, (b) chitosan, and (c) CS1/Fe4 are shown in Fig. 3. The peak appearing at 2θ of 20.0° was assigned to chitosan, while the sharp diffraction peaks in Fe_3O_4 and CS1/Fe4 corresponded to the

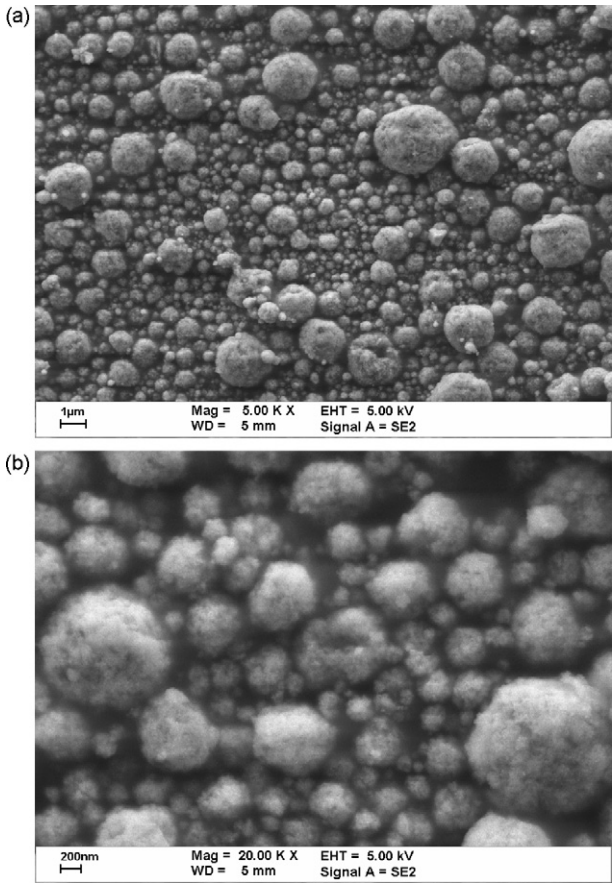

Fig. 4. FESEM images of CS1/Fe4 particles: (a) magnified 5000 times and (b) 20000 times.

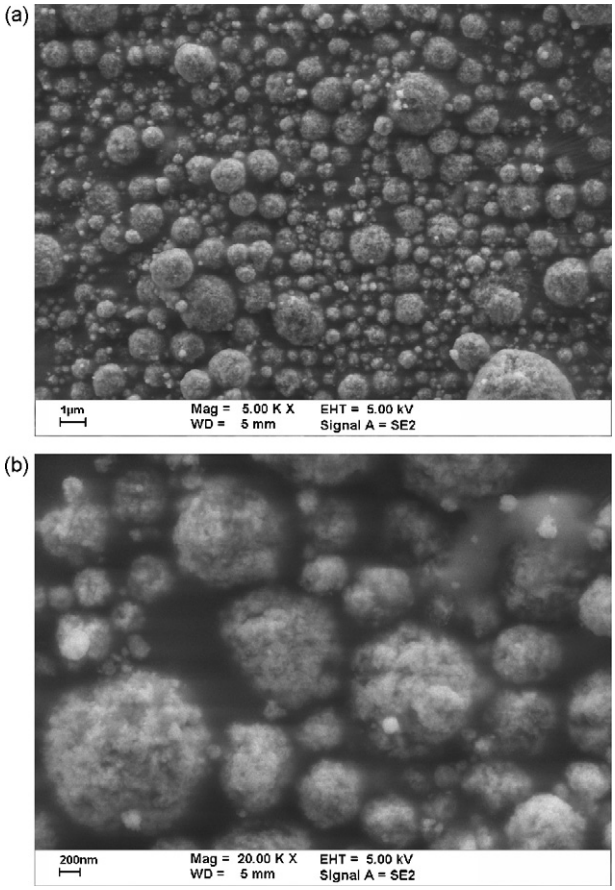

Fig. 5. FESEM images of CS2/Fe4 particles: (a) magnified 5000 times and (b) 20000 times.

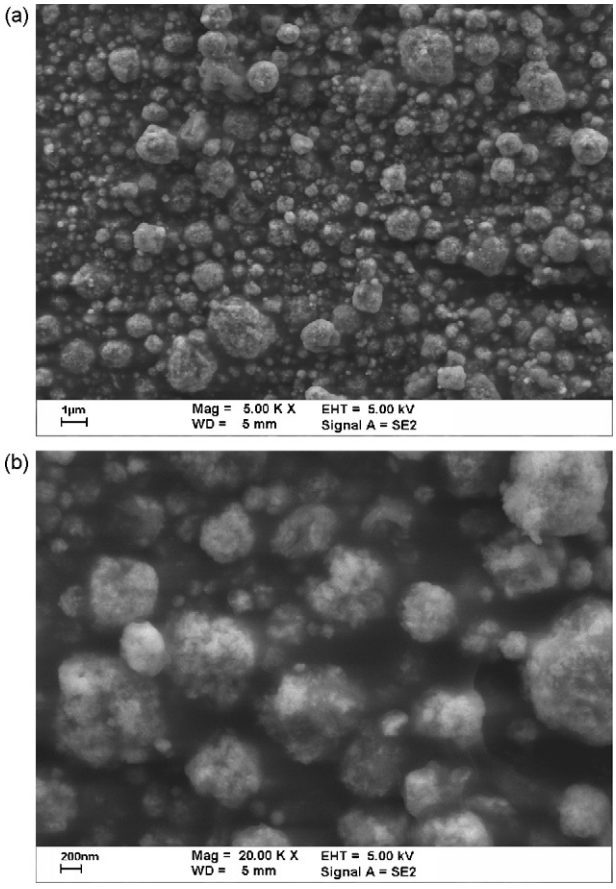

Fig. 6. FESEM images of CS3/Fe4 particles: (a) magnified 5000 times and (b) 20000 times.

scattering from the plane of the magnetite lattice. The ion oxide existing in the CS1/Fe4 was identified as Fe_3O_4. Sharp diffraction peaks are generally obtained from a crystal and a single Fe_3O_4 molecule could not produce a sharp XRD diffraction peak. In the CS1/Fe4, the molar ratio of the chitosan-repeating units to iron atoms was 1:8.8, implying that when Fe_3O_4 was formed under alkali conditions, Fe_3O_4 crystallization occurred at the same time, even if not all of the Fe atoms were chelated with chitosan. During this process, Fe_3O_4 superfine crystals were distributed in the chitosan.

3.3. Morphology of chitosan/iron (II, III) oxide nanoparticles

Figs. 4–6 refer to the FESEM images of CS1/Fe4, CS2/Fe4 and CS3/Fe4, respectively. Figs. 4a, 5a, and 6a show that the magnetic composite nanoparticles took the shape of a spheroid. Their overall surface was quite coarse, as shown in Figs. 4b, 5b, and 6b. The diameters of all particle samples were between 100 nm and 3 μm. For each figure, at least 200 particles were measured for their diameters. As calculated, the average diameters of CS1/Fe4, CS2/Fe4, and CS3/Fe4 were 236 nm, 379 nm and 417 nm, respectively. Along with an increase in chitosan in the samples, the average diameter of the particles likewise increased, and the particle surface became coarser. The irregular micro-level large particles referred to the agglomeration of many small particles sticking into each other. This may have resulted from the increase in concentration of chitosan in the suspension and a higher viscosity of the suspension. In atomizing and drying the samples, it was easy to form large droplets; however, it was not helpful to carry out the evaporation of water, which easily caused mutual collision and the sticking of incompletely dried particles and could lead to the formation of irregular large particles.

3.4. Magnetic properties, zeta potentials and hydrodynamic radii of chitosan/iron (II, III) oxide nanoparticles

Fig. 7a–c show the hysteresis loop of CS1/Fe4, CS2/Fe4 and CS3/Fe4 at 300 K, respectively. The character of ideal superparamagnetic materials is zero coercivity and zero remanence. Fig. 7

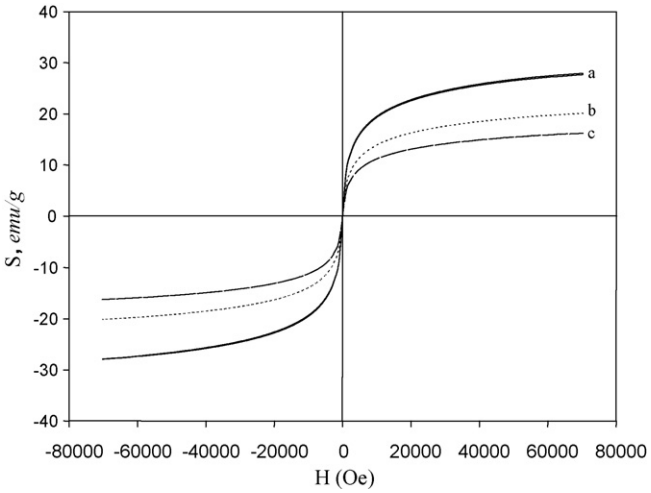

Fig. 7. Hysteresis loop of SQUID of chitosan/iron (II, III) oxide: (a) CS1/Fe4; (b) CS2Fe4; and (c) CS3Fe4.

shows that all samples manifested zero coercivity and zero remanence. Hence, this study concluded that each of the samples had a superparamagnetic property. Along with the increase of chitosan in the samples, their saturated magnetization decreased accordingly. The saturated magnetization rates of CS1/Fe4, CS2/Fe4, and CS3/Fe4 were 27.91 emu/g, 20.09 emu/g and 16.22 emu/g, respectively. The iron content of CS1/Fe4 was 58.42%, and its saturated magnetization was only 27.91 emu/g. Compared with the literature, the saturated magnetization of Fe_3O_4 nanoparticles was above 60 emu/g. Due to the change of chitosan in this study, the saturated magnetization of the product was apparently impacted.

The zeta potential and hydrodynamic diameter of dispersed samples in pure water was measured by DLS. The zeta potential of CSI/Fe4, CS2/Fe4, and CS3/Fe4 was 63.1 mV, 52.5 mV and 48.9 mV, respectively, indicating that the samples could steadily distribute in water. The hydrodynamic diameter calculated from the diffusional properties of CSI/Fe4, CS2/Fe4, and CS3/Fe4 was 3036 nm, 3075 nm and 2981 nm, respectively. As calculated, the ratios of hydrodynamic diameters to the powder FESEM images diameter for CS1/Fe4, CS2/Fe4, and CS3/Fe4 were 12.86, 8.11 and 7.15, respectively. The hydrodynamic diameter of a particle corresponds to the diameter of its dense core, plus the thickness of its salvation layer (e.g., counter-ions moving with the particle). That the ratio tended to decrease with a lower ratio of iron in the formula revealed to the fact that magnetic particles with higher iron content had particles with stronger affinity to other particles in water. This part is worth further study.

4. Conclusions

In summary, a novel method for the preparation of chitosan/iron (II, III) oxide nanoparticles with various ratios of chitosan/iron using the spray-drying method has been reported. In sample CS1/Fe4, AAS results indicated that each chitosan-repeating unit interacted with 8.8 iron atoms or 2.9 Fe_3O_4. AAS results implied that chitosan had strong chelation with Fe; meanwhile, Fe_3O_4 was crystallized and distributed in the chitosan matrix. This was certified by XRD. From the FTIR analysis, it was concluded that the amide and amine deformation bands of samples shifted to lower wavenumbers. This suggested that the amide and/or amine groups from chitosan could be coordinated to the iron ions. FESEM micrographs showed the average particle size of the samples ranging from 200 nm to 500 nm as the content of chitosan increased along with the various formulas. SQUID results indicated the all the samples manifested zero coercivity and zero remanence. This study concluded that each of the samples had a superparamagnetic property. DSL results indicated that all samples could steadily distribute in water. The methods and magnetic nanoparticles described here have provided a novel approach for the preparation of chitosan composite nanoparticles in future works, and one that is worthy of further study and development.

Acknowledgements

This research was financially supported by the National Science Council, Taiwan, R.O.C. under grant no. NSC-96-2313-B-212-002. FESEM assistance from Regional Instruments Center, National Taiwan University, and SQUID assistance from Regional Instruments Center, National Chiao Tung University, are gratefully acknowledged.

References

Arvanitoyannis, I. S. (1999). Totally and partially biodegradable polymer blends on natural and synthetic macromolecules: Preparation, physical properties, and potential as food packing materials. *Journal of Macromolecular Science – Reviews in Macromolecular Chemistry and Physics*, *39*, 205–258.

Arvanitoyannis, I. S., Nakayama, A., & Aiba, S. I. (1998). Chitosan and gelatin based edible films: State diagrams mechanical and permeation properties. *Carbohydrate Polymers*, *37*, 371–382.

Berry, C. C., & Curtis, A. S. G. (2003). Functionalisation of magnetic nanoparticles for applications in biomedicine. *Journal of Physics D: Applied Physics*, *36*, R198–R206.

Carpenter, E. E. (2001). Iron nanoparticles as potential magnetic carriers. *Journal of Magnetism and Magnetic Materials*, *225*, 17–20.

Chatterjee, J., Haik, Y., & Chen, C. J. (2003). Size dependent magnetic properties of iron oxide nanoparticles. *Journal of Magnetism and Magnetic Materials*, *257*, 113–118.

Denkbaş, E. B., Kiliçay, E., Birlikseven, C., & Öztürk, E. (2002). Magnetic chitosan microspheres: Preparation and characterization. *Reactive Functional Polymers*, *50*, 225–232.

Donadel, K., Felisberto, M. D. V., Fàvere, V. T., Rigoni, M., Batistela, N. J., & Laranjeira, M. C. M. (2008). Synthesis and characterization of the iron oxide magnetic particles coated with chitosan biopolymer. *Materials Science & Engineering C*, *28*, 509–514.

Gupta, A. K., & Curtis, A. S. G. (2004). Lactoferrin and ceruloplasmin derivatized superparamagnetic iron oxide nanoparticles for targeting cell surface receptors. *Biomaterial*, *25*, 3029–3040.

Gupta, A. K., & Gupta, M. (2005). Synthesis and surface engineering of iron oxide nanoparticles for biomedical applications. *Biomaterials*, *26*, 3995–4021.

Hong, H., Liu, H., & Wu, W. (2009). Preparation and characterization of chitosan/PEG/gelatin composites for tissue engineering. *Journal of Applied Polymer Science*, *114*, 1220–1225.

Hong, J., Gong, P., Xu, D., Dong, L., & Yao, S. (2007). Stabilization of α-chymotrypsin by covalent immobilization on amine-functionalized superparamagnetic nanogel. *Journal of Biotechnology*, *128*, 597–605.

Huber, D. L. (2005). Synthesis properties and application of iron nanoparticle. *Small*, *5*, 482–501.

Ito, A., Shinkai, M., Honda, H., & Kobayashi, T. (2005). Medical application of functionalized magnetic nanoparticles. *Journal of Bioscience and Bioengineering*, *100*, 1–11.

Jia, Z., Yujun, W., Yangcheng, L., Jingyu, M., & Guangsheng, L. (2006). In site preparation of magnetic chitosan/Fe_3O_4 composite nanoparticles in tiny pools of water-in-oil microemulsion. *Reactive & Functional Polymers*, *66*, 1552–1558.

Jotania, R. B., Khomane, R. B., Chauhan, C. C., Menon, S. K., & Kulkarni, B. D. (2008). Synthesis and magnetic properties of barium–calcium hexaferrite particles prepared by sol–gel and microemulsion techniques. *Journal of Magnetism and Magnetic Materials*, *320*, 1095–1101.

Kim, D. K., Zhang, Y., Voit, W., Rao, K. V., & Muhammed, M. (2001). Synthesis and characterization of surfactant-coated superparamagnetic monodispersed iron oxide nanoparticles. *Journal of Magnetism and Magnetic Materials*, *225*, 30–36.

Kim, E. H., Ahn, Y., & Lee, H. S. (2007). Biomedical applications of superparamagnetic iron oxide nanoparticles encapsulated within chitosan. *Journal of Alloys and Compounds*, *434–435*, 633–636.

Neuberger, T., Schöpf, B., Hofmann, H., Hofmann, M., & Rechenberg, B. V. (2005). Superparamagnetic nanoparticles for biomedical applications: Possibilities and limitations of a new drug delivery system. *Journal of Magnetism and Magnetic Materials*, *293*, 483–496.

Park, J. H., Im, K. H., Lee, S. H., Kim, D. H., Lee, D. Y., Lee, Y. K., et al. (2005). Preparation and characterization of magnetic chitosan particles for hyperthermia application. *Journal of Magnetism and Magnetic Materials*, *293*, 328–333.

Racka, K., Gich, M., Waniewska, A. Ś., Roig, A., & Molins, E. (2005). Magnetic properties of Fe nanoparticles systems. *Journal of Magnetism and Magnetic Materials*, *290–291*, 127–130.

Rellinghaus, B., Stappert, S., Acet, M., & Wassermann, E. F. (2003). Magnetic properties of FePt nanoparticles. *Journal of Magnetism and Magnetic Materials*, *266*, 142–154.

Shahidi, F., Arachchi, J. K. V., & Jeon, Y. J. (1999). Food applications of chitin and chitosans. *Trends in Food Science & Technology*, *10*, 37–51.

Shih, C. M., Twu, Y. K., & Shieh, Y. T. (2006). Chitosan nanoparticles produced by a novel spray drying process. In *Presented at 7th Asia Pacific Chitin–Chitosan Symposium & Exhibition* Busan, Korea, (pp. 335–337).

Storm, G., Belliot, S. O., Daemen, T., & Lasic, D. D. (1995). Surface modification of nanoparticles to oppose uptake by the mononuclear phagocyte system. *Advanced Drug Delivery Reviews*, *17*, 31–48.

Sun, Y. K., Ma, M., Zhang, Y., & Gu, N. (2004). Synthesis of nanometer-size maghemite particles from magnetite. *Colloids and Surfaces A*, *245*, 15–19.

Twu, Y. K., Huang, H. I., Chang, S. Y., & Wang, S. L. (2003). Preparation and sorption activity of chitosan/cellulose blend beads. *Carbohydrate Polymers*, *54*, 425–430.

Wang, S., Liu, W., Han, B., & Yang, L. (2009). Study on a hydroxypropyl chitosan-gelatin based scaffold for corneal stroma tissue engineering. *Applied Surface Science*, *255*, 8701–8705.

Xu, C., & Sun, S. (2007). Monodisperse magnetic nanoparticles for biomedical applications. *Polymer International*, *56*, 821–826.

Yan, G. P., Robinson, L., & Hogg, P. (2007). Magnetic resonance imaging contrast agents: Overview and perspectives. *Radiography*, *13*, 5–19.

Yen, M. T., Yang, J. H., & Mau, J. L. (2008). Antioxidant properties of chitosan from crab shells. *Carbohydrate Polymers*, *74*, 840–844.

Zhang, J., Zhang, S., Wang, Y., & Zeng, J. (2007). Composite magnetic microspheres: Preparation and characterization. *Journal of Magnetism and Magnetic Materials*, *309*, 197–201.